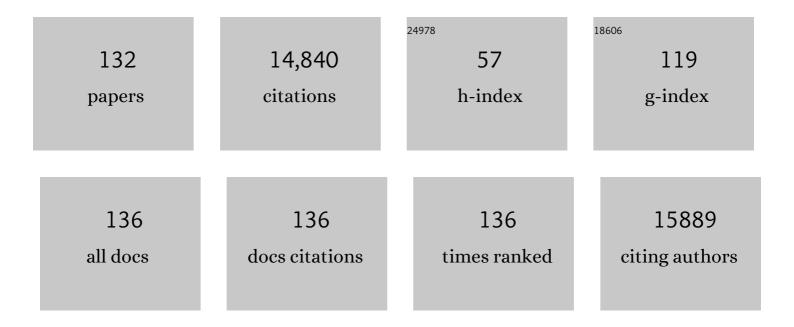
List of Publications by Year in descending order

Source: https://exaly.com/author-pdf/3415790/publications.pdf Version: 2024-02-01



#	Article	IF	CITATIONS
1	Two-dimensional porous Cu-CuO nanosheets: Integration of heterojunction and morphology engineering to achieve high-effective and stable reduction of the aromatic nitro-compounds. Chinese Chemical Letters, 2023, 34, 107295.	4.8	7
2	A dual-active Co-CoO heterojunction coupled with Ti3C2-MXene for highly-performance overall water splitting. Nano Research, 2022, 15, 238-247.	5.8	66
3	Vanadiumâ€Incorporated CoP <sub>2</sub> with Lattice Expansion for Highly Efficient Acidic Overall Water Splitting. Angewandte Chemie, 2022, 134, .	1.6	16
4	Multi-touch cobalt phosphide-tungsten phosphide heterojunctions anchored on reduced graphene oxide boosting wide pH hydrogen evolution. Science China Materials, 2022, 65, 1225-1236.	3.5	21
5	Vanadiumâ€Incorporated CoP <sub>2</sub> with Lattice Expansion for Highly Efficient Acidic Overall Water Splitting. Angewandte Chemie - International Edition, 2022, 61, .	7.2	85
6	Integration of heterointerface and porosity engineering to achieve efficient hydrogen evolution of 2D porous NiMoN nanobelts coupled with Ni particles. Electrochimica Acta, 2022, 403, 139702.	2.6	12
7	Ni-promoted MoS <sub>2</sub> in hollow zeolite nanoreactors: enhanced catalytic activity and stability for deep hydrodesulfurization. Journal of Materials Chemistry A, 2022, 10, 7263-7270.	5.2	8
8	The Fe <sub>3</sub> C–N <sub><i>x</i></sub> Site Assists the Fe–N <sub><i>x</i></sub> Site to Promote Activity of the Fe–N–C Electrocatalyst for Oxygen Reduction Reaction. ACS Sustainable Chemistry and Engineering, 2022, 10, 3346-3354.	3.2	15
9	Ultrathin Porous Carbon Nitride Bundles with an Adjustable Energy Band Structure toward Simultaneous Solar Photocatalytic Water Splitting and Selective Phenylcarbinol Oxidation. Angewandte Chemie, 2021, 133, 4865-4872.	1.6	19
10	Twoâ€Dimensional Porous Molybdenum Phosphide/Nitride Heterojunction Nanosheets for pHâ€Universal Hydrogen Evolution Reaction. Angewandte Chemie - International Edition, 2021, 60, 6673-6681.	7.2	227
11	Ultrathin Porous Carbon Nitride Bundles with an Adjustable Energy Band Structure toward Simultaneous Solar Photocatalytic Water Splitting and Selective Phenylcarbinol Oxidation. Angewandte Chemie - International Edition, 2021, 60, 4815-4822.	7.2	233
12	One-dimensional CO9S8-V3S4 heterojunctions as bifunctional electrocatalysts for highly efficient overall water splitting. Science China Materials, 2021, 64, 1396-1407.	3.5	36
13	Moltenâ€Salt Technology Application for the Synthesis of Photocatalytic Materials. Energy Technology, 2021, 9, 2000945.	1.8	9
14	2D porous molybdenum nitride/cobalt nitride heterojunction nanosheets with interfacial electron redistribution for effective electrocatalytic overall water splitting. Journal of Materials Chemistry A, 2021, 9, 8620-8629.	5.2	72
15	2D thin sheets composed of Co <sub>5.47</sub> N–MgO embedded in carbon as a durable catalyst for the reduction of aromatic nitro compounds. Materials Chemistry Frontiers, 2021, 5, 2798-2809.	3.2	7
16	Twoâ€Dimensional Porous Molybdenum Phosphide/Nitride Heterojunction Nanosheets for pHâ€Universal Hydrogen Evolution Reaction. Angewandte Chemie, 2021, 133, 6747-6755.	1.6	25
17	Innenrücktitelbild: Ultrathin Porous Carbon Nitride Bundles with an Adjustable Energy Band Structure toward Simultaneous Solar Photocatalytic Water Splitting and Selective Phenylcarbinol Oxidation (Angew. Chem. 9/2021). Angewandte Chemie, 2021, 133, 5003-5003.	1.6	1
18	Operando Cooperated Catalytic Mechanism of Atomically Dispersed Cuâ^'N 4 and Znâ^'N 4 for Promoting Oxygen Reduction Reaction. Angewandte Chemie, 2021, 133, 14124-14131.	1.6	22

#	Article	IF	CITATIONS
19	Operando Cooperated Catalytic Mechanism of Atomically Dispersed Cuâ^'N <sub>4</sub> and Znâ''N <sub>4</sub> for Promoting Oxygen Reduction Reaction. Angewandte Chemie - International Edition, 2021, 60, 14005-14012.	7.2	312
20	Insight on the active sites of CoNi alloy embedded in N-doped carbon nanotubes for oxygen reduction reaction. Science China Materials, 2021, 64, 2719-2728.	3.5	16
21	Electronic Structure Modulation of Nonâ€Nobleâ€Metalâ€Based Catalysts for Biomass Electrooxidation Reactions. Small Structures, 2021, 2, 2100095.	6.9	28
22	Hollow CoP spheres assembled from porous nanosheets as high-rate and ultra-stable electrodes for advanced supercapacitors. Journal of Materials Chemistry A, 2021, 9, 26226-26235.	5.2	31
23	Znâ€Doped Porous CoNiP Nanosheet Arrays as Efficient and Stable Bifunctional Electrocatalysts for Overall Water Splitting. Energy Technology, 2020, 8, 1901079.	1.8	20
24	Cubic imidazolate frameworks-derived CoFe alloy nanoparticles-embedded N-doped graphitic carbon for discharging reaction of Zn-air battery. Science China Materials, 2020, 63, 327-338.	3.5	51
25	Promoting the spatial charge separation by building porous ZrO2@TiO2 heterostructure toward photocatalytic hydrogen evolution. Journal of Colloid and Interface Science, 2020, 561, 568-575.	5.0	23
26	A Singleâ€Source Precursor Route toward Smallâ€Sized Nickel Particles Embedded into SiO 2 Sheet as Magnetic Separable Catalyst. ChemistrySelect, 2020, 5, 11708-11712.	0.7	1
27	Porous cobalt/tungsten nitride polyhedra as efficient bifunctional electrocatalysts for overall water splitting. Journal of Materials Chemistry A, 2020, 8, 22938-22946.	5.2	56
28	In situ intercalation and exploitation of Co3O4 nanoparticles grown on carbon nitride nanosheets for highly efficient degradation of methylene blue. Dalton Transactions, 2020, 49, 14665-14672.	1.6	12
29	Facile immobilization of polyoxometalates for low-cost molybdenum/tungsten phosphide nanoparticles on carbon black for efficient electrocatalytic hydrogen evolution. Journal of Coordination Chemistry, 2020, 73, 2590-2601.	0.8	3
30	Electronic Tuning of Ni by Mo Species for Highly Efficient Hydroisomerization of <i>n</i> -Alkanes Comparable to Pt-Based Catalysts. ACS Catalysis, 2020, 10, 10449-10458.	5.5	63
31	Porous Plate-like MoP Assembly as an Efficient pH-Universal Hydrogen Evolution Electrocatalyst. ACS Applied Materials & Interfaces, 2020, 12, 49596-49606.	4.0	46
32	Surface curvature-confined strategy to ultrasmall nickel-molybdenum sulfide nanoflakes for highly efficient deep hydrodesulfurization. Nano Research, 2020, 13, 882-890.	5.8	22
33	Interfacial Engineering of MoO <sub>2</sub> â€FeP Heterojunction for Highly Efficient Hydrogen Evolution Coupled with Biomass Electrooxidation. Advanced Materials, 2020, 32, e2000455.	11.1	401
34	A Promoted Charge Separation/Transfer System from Cu Single Atoms and C <sub>3</sub> N <sub>4</sub> Layers for Efficient Photocatalysis. Advanced Materials, 2020, 32, e2003082.	11.1	333
35	Cobalt nanoparticles decorated on nitrogen-doped graphene as excellent electromagnetic wave absorbent in Ku-band. Journal of Materials Science: Materials in Electronics, 2020, 31, 12044-12055.	1.1	4
36	A "competitive occupancy―strategy toward Co–N <sub>4</sub> single-atom catalysts embedded in 2D TiN/rGO sheets for highly efficient and stable aromatic nitroreduction. Journal of Materials Chemistry A, 2020, 8, 4807-4815.	5.2	19

#	Article	IF	CITATIONS
37	An effective "precursor-transformation―route toward the high-yield synthesis of ZIF-8 tubes. Chemical Communications, 2020, 56, 2913-2916.	2.2	35
38	In situ immobilization of ultra-fine Ag NPs onto magnetic Ag@RF@Fe3O4 core-satellite nanocomposites for the rapid catalytic reduction of nitrophenols. Water Research, 2020, 179, 115882.	5.3	87
39	TiO2-on-C3N4 double-shell microtubes: In-situ fabricated heterostructures toward enhanced photocatalytic hydrogen evolution. Journal of Colloid and Interface Science, 2020, 572, 22-30.	5.0	46
40	Effective Electrocatalytic Hydrogen Evolution in Neutral Medium Based on 2D MoP/MoS <sub>2</sub> Heterostructure Nanosheets. ACS Applied Materials & Interfaces, 2019, 11, 25986-25995.	4.0	86
41	B,N-Doped Defective Carbon Entangled Fe <sub>3</sub> C Nanoparticles as the Superior Oxygen Reduction Electrocatalyst for Zn–Air Batteries. ACS Sustainable Chemistry and Engineering, 2019, 7, 19104-19112.	3.2	48
42	3D hierarchical V–Ni-based nitride heterostructure as a highly efficient pH-universal electrocatalyst for the hydrogen evolution reaction. Journal of Materials Chemistry A, 2019, 7, 15823-15830.	5.2	100
43	Co Nanoislands Rooted on Co–N–C Nanosheets as Efficient Oxygen Electrocatalyst for Zn–Air Batteries. Advanced Materials, 2019, 31, e1901666.	11.1	455
44	Anionâ€Modulated HER and OER Activities of 3D Ni–Vâ€Based Interstitial Compound Heterojunctions for Highâ€Efficiency and Stable Overall Water Splitting. Advanced Materials, 2019, 31, e1901174.	11.1	479
45	Cobalt Nickel Nitrogen Array as a Easily Eecoverable, Effective Catalyst for Liquidâ€Phase Catalytic Reaction with Remarkable Recycled Stability. ChemistrySelect, 2019, 4, 3515-3523.	0.7	3
46	Porous NiCoP nanowalls as promising electrode with high-area and mass capacitance for supercapacitors. Science China Materials, 2019, 62, 1115-1126.	3.5	42
47	CoO-Mo2N hollow heterostructure for high-efficiency electrocatalytic hydrogen evolution reaction. NPG Asia Materials, 2019, 11, .	3.8	65
48	N-doped carbon-coated Co3O4 nanosheet array/carbon cloth for stable rechargeable Zn-air batteries. Science China Materials, 2019, 62, 624-632.	3.5	34
49	Molecule Self-Assembly Synthesis of Porous Few-Layer Carbon Nitride for Highly Efficient Photoredox Catalysis. Journal of the American Chemical Society, 2019, 141, 2508-2515.	6.6	685
50	Clusterâ€like Co <sub>4</sub> N embedded into carbon sphere as an efficient, magneticâ€separated catalyst for catalytic hydrogenation. ChemistrySelect, 2019, 4, 90-99.	0.7	7
51	Trace Pt Clusters Dispersed on SAPOâ€1 1 Promoting the Synergy of Metal Sites with Acid Sites for Highâ€Effective Hydroisomerization of <i>n</i> â€Alkanes. Small Methods, 2019, 3, 1800510.	4.6	34
52	Ni <sub>2</sub> P Entwined by Graphite Layers as a Low-Pt Electrocatalyst in Acidic Media for Oxygen Reduction. ACS Applied Materials & Interfaces, 2018, 10, 9999-10010.	4.0	34
53	Trapping [PMo <sub>12</sub> O <sub>40</sub> ] <sup>3â^`</sup> clusters into pre-synthesized ZIF-67 toward Mo <sub>x</sub> Co <sub>x</sub> C particles confined in uniform carbon polyhedrons for efficient overall water splitting. Chemical Science, 2018, 9, 4746-4755.	3.7	189
54	Cobalt-vanadium bimetal-based nanoplates for efficient overall water splitting. Science China Materials, 2018, 61, 80-90.	3.5	52

#	Article	IF	CITATIONS
55	Ni <sub>3</sub> S <sub>2</sub> Nanosheets in Situ Epitaxially Grown on Nanorods as High Active and Stable Homojunction Electrocatalyst for Hydrogen Evolution Reaction. ACS Sustainable Chemistry and Engineering, 2018, 6, 2474-2481.	3.2	72
56	Synergism of molybdenum nitride and palladium for high-efficiency formic acid electrooxidation. Journal of Materials Chemistry A, 2018, 6, 7623-7630.	5.2	54
57	Integrating the active OER and HER components as the heterostructures for the efficient overall water splitting. Nano Energy, 2018, 44, 353-363.	8.2	516
58	Holey Reduced Graphene Oxide Coupled with an Mo <sub>2</sub> N–Mo <sub>2</sub> C Heterojunction for Efficient Hydrogen Evolution. Advanced Materials, 2018, 30, 1704156.	11.1	459
59	A Stable Bifunctional Catalyst for Rechargeable Zinc–Air Batteries: Iron–Cobalt Nanoparticles Embedded in a Nitrogenâ€Doped 3D Carbon Matrix. Angewandte Chemie - International Edition, 2018, 57, 16166-16170.	7.2	365
60	A "MOFs plus MOFs―strategy toward Co–Mo <sub>2</sub> N tubes for efficient electrocatalytic overall water splitting. Journal of Materials Chemistry A, 2018, 6, 20100-20109.	5.2	131
61	A Stable Bifunctional Catalyst for Rechargeable Zinc–Air Batteries: Iron–Cobalt Nanoparticles Embedded in a Nitrogenâ€Doped 3D Carbon Matrix. Angewandte Chemie, 2018, 130, 16398-16402.	1.6	64
62	Porous NiCoP nanosheets as efficient and stable positive electrodes for advanced asymmetric supercapacitors. Journal of Materials Chemistry A, 2018, 6, 17905-17914.	5.2	189
63	Assembly of TiO2 ultrathin nanosheets with surface lattice distortion for solar-light-driven photocatalytic hydrogen evolution. Applied Catalysis B: Environmental, 2018, 239, 317-323.	10.8	77
64	Highâ€Efficient, Stable Electrocatalytic Hydrogen Evolution in Acid Media by Amorphous Fe <i><sub>x</sub></i> P Coating Fe <sub>2</sub> N Supported on Reduced Graphene Oxide. Small, 2018, 14, e1801717.	5.2	72
65	2-D porous Ni <sub>3</sub> N–Co <sub>3</sub> N hybrids derived from ZIF-67/Ni(OH) <sub>2</sub> sheets as a magnetically separable catalyst for hydrogenation reactions. Chemical Communications, 2018, 54, 11088-11091.	2.2	33
66	Hierarchical porous NiCo <sub>2</sub> O <sub>4</sub> nanosheet arrays directly grown on carbon cloth with superior lithium storage performance. Dalton Transactions, 2017, 46, 4717-4723.	1.6	32
67	A general strategy toward the large-scale synthesis of the noble metal-oxide nanocrystal hybrids with intimate interfacial contact for the catalytic reduction of p-nitrophenol and photocatalytic degradation of pollutants. Research on Chemical Intermediates, 2017, 43, 4759-4779.	1.3	4
68	Promising biomass-derived hierarchical porous carbon material for high performance supercapacitor. RSC Advances, 2017, 7, 10385-10390.	1.7	46
69	Gelatin-assisted synthesis of ZnS hollow nanospheres: the microstructure tuning, formation mechanism and application for Pt-free photocatalytic hydrogen production. CrystEngComm, 2017, 19, 461-468.	1.3	17
70	Layer Stacked Iodine and Phosphorus Coâ€doped C <sub>3</sub> N <sub>4</sub> for Enhanced Visibleâ€Light Photocatalytic Hydrogen Evolution. ChemCatChem, 2017, 9, 4083-4089.	1.8	36
71	Inorganic acid-derived hydrogen-bonded organic frameworks to form nitrogen-rich carbon nitrides for photocatalytic hydrogen evolution. Journal of Materials Chemistry A, 2017, 5, 21979-21985.	5.2	69
72	Self-supported Ni6MnO8 3D mesoporous nanosheet arrays with ultrahigh lithium storage properties and conversion mechanism by in-situ XAFS. Nano Research, 2017, 10, 263-275.	5.8	23

#	Article	IF	CITATIONS
73	Synergistic Effect of Tungsten Nitride and Palladium for the Selective Hydrogenation of Cinnamaldehyde at the C=C bond. ChemCatChem, 2016, 8, 1718-1726.	1.8	26
74	Phosphorusâ€Doped Carbon Nitride Tubes with a Layered Microâ€nanostructure for Enhanced Visibleâ€Light Photocatalytic Hydrogen Evolution. Angewandte Chemie - International Edition, 2016, 55, 1830-1834.	7.2	869
75	Phosphorusâ€Doped Carbon Nitride Tubes with a Layered Microâ€nanostructure for Enhanced Visibleâ€Light Photocatalytic Hydrogen Evolution. Angewandte Chemie, 2016, 128, 1862-1866.	1.6	173
76	Graphene-like nanocomposites anchored by Ni <sub>3</sub> S <sub>2</sub> slices for Li-ion storage. RSC Advances, 2016, 6, 48083-48088.	1.7	23
77	Constructing B and N separately co-doped carbon nanocapsules-wrapped Fe/Fe <sub>3</sub> C for oxygen reduction reaction with high current density. Physical Chemistry Chemical Physics, 2016, 18, 26572-26578.	1.3	12
78	A hybridized heterojunction structure between TiO2nanorods and exfoliated graphitic carbon-nitride sheets for hydrogen evolution under visible light. CrystEngComm, 2016, 18, 6875-6880.	1.3	13
79	In situ synthesis, enhanced luminescence and application in dye sensitized solar cells of Y2O3/Y2O2S:Eu3+ nanocomposites by reduction of Y2O3:Eu3+. Scientific Reports, 2016, 6, 37133.	1.6	38
80	An effective poly(p-phenylenevinylene) polymer adhesion route toward three-dimensional nitrogen-doped carbon nanotube/reduced graphene oxide composite for direct electrocatalytic oxygen reduction. Nano Research, 2016, 9, 3364-3376.	5.8	19
81	Cluster-like molybdenum phosphide anchored on reduced graphene oxide for efficient hydrogen evolution over a broad pH range. Chemical Communications, 2016, 52, 9530-9533.	2.2	102
82	Small-sized tungsten nitride anchoring into a 3D CNT-rGO framework as a superior bifunctional catalyst for the methanol oxidation and oxygen reduction reactions. Nano Research, 2016, 9, 329-343.	5.8	75
83	A "1-methylimidazole-fixation―route to anchor small-sized nitrides on carbon supports as non-Pt catalysts for the hydrogen evolution reaction. RSC Advances, 2016, 6, 29303-29307.	1.7	29
84	Synergistic effect of Mo <sub>2</sub> N and Pt for promoted selective hydrogenation of cinnamaldehyde over Pt–Mo <sub>2</sub> N/SBA-15. Catalysis Science and Technology, 2016, 6, 2403-2412.	2.1	58
85	GO-induced assembly of gelatin toward stacked layer-like porous carbon for advanced supercapacitors. Nanoscale, 2016, 8, 2418-2427.	2.8	69
86	A Platinum–Vanadium Nitride/Porous Graphitic Nanocarbon Composite as an Excellent Catalyst for the Oxygen Reduction Reaction. ChemElectroChem, 2015, 2, 1813-1820.	1.7	14
87	ZnO-dotted porous ZnS cluster microspheres for high efficient, Pt-free photocatalytic hydrogen evolution. Scientific Reports, 2015, 5, 8858.	1.6	34
88	From graphite to porous graphene-like nanosheets for high rate lithium-ion batteries. Nano Research, 2015, 8, 2998-3010.	5.8	76
89	A novel Fe <sub>3</sub> C/graphitic carbon composite with electromagnetic wave absorption properties in the C-band. RSC Advances, 2015, 5, 60135-60140.	1.7	45
90	A hierarchical porous carbon material from a loofah sponge network for high performance supercapacitors. RSC Advances, 2015, 5, 42430-42437.	1.7	86

#	Article	IF	CITATIONS
91	Phosphorusâ€Modified Tungsten Nitride/Reduced Graphene Oxide as a Highâ€Performance, Nonâ€Nobleâ€Metal Electrocatalyst for the Hydrogen Evolution Reaction. Angewandte Chemie - International Edition, 2015, 54, 6325-6329.	7.2	515
92	Silica direct evaporation: a size-controlled approach to SiC/carbon nanosheet composites as Pt catalyst supports for superior methanol electrooxidation. Journal of Materials Chemistry A, 2015, 3, 24139-24147.	5.2	20
93	Nitrogen-doped graphene supported Pd@PdO core-shell clusters for C-C coupling reactions. Nano Research, 2014, 7, 1280-1290.	5.8	66
94	Heterojunction Ag–TiO <sub>2</sub> Nanopillars for Visibleâ€Lightâ€Driven Photocatalytic H <sub>2</sub> Production. ChemPlusChem, 2014, 79, 995-1000.	1.3	15
95	Hierarchical composites of TiO2 nanowire arrays on reduced graphene oxide nanosheets with enhanced photocatalytic hydrogen evolution performance. Journal of Materials Chemistry A, 2014, 2, 4366-4374.	5.2	112
96	In situ growth of Bi <sub>2</sub> MoO <sub>6</sub> on reduced graphene oxide nanosheets for improved visible-light photocatalytic activity. CrystEngComm, 2014, 16, 842-849.	1.3	80
97	Intermittent microwave heating-promoted rapid fabrication of sheet-like Ag assemblies and small-sized Ag particles and their use as co-catalyst of ZnO for enhanced photocatalysis. Journal of Materials Chemistry A, 2014, 2, 3015.	5.2	19
98	A New Combustion Route to Synthesize Mixed Valence Vanadium Oxide Heterojunction Composites as Visibleâ€Lightâ€Driven Photocatalysts. ChemCatChem, 2014, 6, 2553-2559.	1.8	12
99	Small-sized and high-dispersed WN from [SiO <sub>4</sub> (W <sub>3</sub> O <sub>9</sub> 1 <sub>4</sub> ] <sup>4â^'</sup> clusters loading on GO-derived graphene as promising carriers for methanol electro-oxidation. Energy and Environmental Science. 2014. 7. 1939-1949.	15.6	130
100	Isolated Boron and Nitrogen Sites on Porous Graphitic Carbon Synthesized from Nitrogen ontaining Chitosan for Supercapacitors. ChemSusChem, 2014, 7, 1637-1646.	3.6	128
101	B and N isolate-doped graphitic carbon nanosheets from nitrogen-containing ion-exchanged resins for enhanced oxygen reduction. Scientific Reports, 2014, 4, 5184.	1.6	68
102	Growth of small sized CeO2 particles in the interlayers of expanded graphite for high-performance room temperature NOx gas sensors. Journal of Materials Chemistry A, 2013, 1, 12742.	5.2	96
103	A Floating Porous Crystalline TiO <sub>2</sub> Ceramic with Enhanced Photocatalytic Performance for Wastewater Decontamination. European Journal of Inorganic Chemistry, 2013, 2013, 2411-2417.	1.0	59
104	Single-step pyrolytic preparation of Mo2C/graphitic carbon nanocomposite as catalyst carrier for the direct liquid-feed fuel cells. RSC Advances, 2013, 3, 4771.	1.7	27
105	Facile synthesis and shape control of Fe3O4 nanocrystals with good dispersion and stabilization. CrystEngComm, 2013, 15, 3366.	1.3	19
106	Hierarchical flake-like Bi2MoO6/TiO2 bilayer films for visible-light-induced self-cleaning applications. Journal of Materials Chemistry A, 2013, 1, 6961.	5.2	102
107	A novel Ag/graphene composite: facile fabrication and enhanced antibacterial properties. Journal of Materials Science, 2013, 48, 1980-1985.	1.7	40
108	Hierarchical Composite of Ag/AgBr Nanoparticles Supported on Bi <sub>2</sub> MoO <sub>6</sub> Hollow Spheres for Enhanced Visible‣ight Photocatalytic Performance. ChemPlusChem, 2013, 78, 117-123.	1.3	58

#	Article	IF	CITATIONS
109	Confinement Effect on Ag Clusters in the Channels of Wellâ€Ordered Mesoporous TiO <sub>2</sub> and their Enhanced Photocatalytic Performance. ChemCatChem, 2013, 5, 1354-1358.	1.8	13
110	Inâ€Situ Fabrication of Ag/Ag <sub>3</sub> PO <sub>4</sub> /Graphene Triple Heterostructure Visibleâ€Light Photocatalyst through Grapheneâ€Assisted Reduction Strategy. ChemCatChem, 2013, 5, 1359-1367.	1.8	54
111	Facile synthesis of sheet-like ZnO assembly composed of small ZnO particles for highly efficient photocatalysis. Journal of Materials Chemistry A, 2013, 1, 5700.	5.2	170
112	A facile and green synthesis route towards two-dimensional TiO2@Ag heterojunction structure with enhanced visible light photocatalytic activity. CrystEngComm, 2013, 15, 5821.	1.3	25
113	From coconut shell to porous graphene-like nanosheets for high-power supercapacitors. Journal of Materials Chemistry A, 2013, 1, 6462.	5.2	794
114	Cost-effective large-scale synthesis of ZnO photocatalyst with excellent performance for dye photodegradation. Chemical Communications, 2012, 48, 2858.	2.2	515
115	Highly dispersed Ni-decorated porous hollow carbon nanofibers: fabrication, characterization, and NOx gas sensors at room temperature. Journal of Materials Chemistry, 2012, 22, 24814.	6.7	35
116	Controlled synthesis of thorny anatase TiO <sub>2</sub> tubes for construction of Ag–AgBr/TiO <sub>2</sub> composites as highly efficient simulated solar-light photocatalyst. Journal of Materials Chemistry, 2012, 22, 2081-2088.	6.7	84
117	NaYF4:Er3+/Yb3+–graphene composites: preparation, upconversion luminescence, and application in dye-sensitized solar cells. Journal of Materials Chemistry, 2012, 22, 20381.	6.7	63
118	A novel soft template strategy to fabricate mesoporous carbon/graphene composites as high-performance supercapacitor electrodes. RSC Advances, 2012, 2, 8359.	1.7	82
119	A facile one-pot route for the controllable growth of small sized and well-dispersed ZnO particles on GO-derived graphene. Journal of Materials Chemistry, 2012, 22, 11778.	6.7	159
120	Nitrogen-doped graphene with high nitrogen level via a one-step hydrothermal reaction of graphene oxide with urea for superior capacitive energy storage. RSC Advances, 2012, 2, 4498.	1.7	696
121	In Situ Reduction, Oxygen Etching, and Reduction Using Formic Acid: An Effective Strategy for Controllable Growth of Monodisperse Palladium Nanoparticles on Graphene. ChemPlusChem, 2012, 77, 301-307.	1.3	18
122	Fabrication of a 3D Hierarchical Flower‣ike MgO Microsphere and Its Application as Heterogeneous Catalyst. European Journal of Inorganic Chemistry, 2012, 2012, 954-960.	1.0	27
123	Graphitic Carbon Nanocapsules: Scaled Preparation, Formation Mechanism, and Use as an Excellent Support for Methanol Electro-oxidation. European Journal of Inorganic Chemistry, 2012, 2012, 961-968.	1.0	13
124	An effective strategy for small-sized and highly-dispersed palladium nanoparticles supported on graphene with excellent performance for formic acid oxidation. Journal of Materials Chemistry, 2011, 21, 3384.	6.7	235
125	Facile solvothermal synthesis of hierarchical flower-like Bi <sub>2</sub> MoO <sub>6</sub> hollow spheres as high performance visible-light driven photocatalysts. Journal of Materials Chemistry, 2011, 21, 887-892.	6.7	427
126	Magnetically separable porous graphitic carbon with large surface area as excellent adsorbents for metal ions and dye. Journal of Materials Chemistry, 2011, 21, 7232.	6.7	85

#	Article	IF	CITATIONS
127	3D hierarchical flower-like TiO2 nanostructure: morphology control and its photocatalytic property. CrystEngComm, 2011, 13, 2994.	1.3	237
128	Oneâ€pot synthesis of silver particle aggregation as highly active SERS substrate. Journal of Raman Spectroscopy, 2011, 42, 5-11.	1.2	19
129	Wellâ€Ordered Largeâ€Pore Mesoporous Anatase TiO <sub>2</sub> with Remarkably High Thermal Stability and Improved Crystallinity: Preparation, Characterization, and Photocatalytic Performance. Advanced Functional Materials, 2011, 21, 1922-1930.	7.8	431
130	Solvothermal Synthesis, Characterization, and Formation Mechanism of a Single‣ayer Anatase TiO <sub>2</sub> Nanosheet with a Porous Structure. European Journal of Inorganic Chemistry, 2011, 2011, 754-760.	1.0	22
131	Dyeâ€Sensitised Solar Cells Based on Largeâ€Pore Mesoporous TiO <sub>2</sub> with Controllable Pore Diameters. European Journal of Inorganic Chemistry, 2011, 2011, 4730-4737.	1.0	12
132	Simple Strategy for Preparation of Core Colloids Modified with Metal Nanoparticles. Journal of Physical Chemistry C, 2007, 111, 3651-3657.	1.5	87